Construction and Building Materials 344 (2022) 128272

Contents lists available at ScienceDirect

Construction and Building Materials

journal homepage: www.elsevier.com/locate/conbuildmat

Evaluation of self-healing in cementitious materials with superabsorbent polymers through ultrasonic mapping

Gerlinde Lefever [a,*], Danny Van Hemelrijck [a], Dimitrios G. Aggelis [a], Didier Snoeck [a,b]

[a] Department Mechanics of Materials and Constructions, Vrije Universiteit Brussel (VUB), Pleinlaan 2, 1050 Brussels, Belgium
[b] BATir Department, Université Libre de Bruxelles (ULB), 50 F.D. Roosevelt Avenue, 1050 Brussels, Belgium

ARTICLE INFO

Keywords:
Cement
Self-healing
Ultrasound
Superabsorbent polymer (SAP)
Hydrogel

ABSTRACT

The maintenance and repair of concrete infrastructure covers an increasing portion of the annual construction budget. For this reason, self-healing cementitious materials have been investigated thoroughly in literature. One way to achieve an effective self-healing composite is by promoting their inherent repair ability through the inclusion of superabsorbent polymers (SAPs). Thanks to their large absorption capacity upon contact with water, SAPs allow to preserve the humidity inside the cracks for a longer period of time, which is essential to promote the autogenous healing process. In order to encourage the application of SAPs for self-healing purposes, adequate assessment techniques should be at hand in order to evaluate a SAP's effectiveness for self-repair. Whereas various methods, such as water permeability tests and microscopic analysis, are used to assess a material's self-healing potential, mechanical tests are needed to determine the regain in mechanical performance. Due to the destructive nature of these methods, the monitoring of the self-healing mechanism over time is practically impossible. In the present research, a non-destructive testing methodology based on ultrasonic wave through transmission was investigated, due to its sensitivity to the elastic properties of the material under study. By means of ultrasonic mapping, the interior was visualized and allowed to determine the degree and uniformity of healing along the depth for different healing times for the first time in literature.

1. Introduction

Concrete is one of the most widely used construction materials, owing to its high compressive strength. On the other hand, its tensile capacity is relatively low, which makes concrete prone to cracking. To safeguard the durability and mechanical performance of structural elements, these cracks should be repaired in a timely manner. At the present time, the maintenance and repair of concrete structures already covers a large portion of the construction budget and this is only expected to increase as these structures are ageing. Additionally, the limited accessibility of some structural components makes it practically impossible for manual repairs to be carried out. A solution could be found through the introduction of self-healing cementitious composites. The advantage of self-healing mixtures compared to the conventional repair techniques lies in the automatic activation of the healing mechanism, omitting inspections as well as labour-intensive and costly repairs. Cementitious materials possess an inherent ability to repair damage through so-called autogenous healing. The main mechanisms that contribute to the self-healing capacity are the continued hydration and the calcium carbonate precipitation. The former process consists in the further hydration of unhydrated cement particles that are present inside the crack upon contact with water. The precipitation of $CaCO_3$ is caused by the dissolution and carbonation of CH [1,2]. Both mechanisms occur simultaneously, though the continued hydration mostly takes place at early age until the unhydrated cement is consumed. The precipitation of $CaCO_3$ then becomes more prominent at later ages [3]. An important factor for these reactions to take place is the availability of water inside the cracks. Hence, an improvement of the autogenous healing mechanism can be achieved by introducing a more continuous water supply within the matrix material. In this respect, the addition of superabsorbent polymers (SAPs) to cementitious mixtures was investigated [4,5,6,7]. SAPs are capable to absorb and retain large amounts of water. When water or moisture tries to enter the crack, the SAPs present inside the crack will swell upon absorption of the water, thereby physically blocking the crack entrance (self-sealing). During dry periods, the water from the SAPs is released and induces the deposition of healing products through the continued hydration and calcium carbonate precipitation (self-healing).

* Corresponding author.
E-mail address: Gerlinde.Lefever@vub.be (G. Lefever).

https://doi.org/10.1016/j.conbuildmat.2022.128272
Received 11 April 2022; Received in revised form 20 June 2022; Accepted 26 June 2022
Available online 1 July 2022

To advocate the implementation of self-healing cementitious materials in construction industry, an evaluation of the self-healing effectiveness is highly important to ensure a structure's safety. A distinction should be made between the assessment techniques that evaluate the filling, the sealing and the healing of cracks. The filling or visual crack closure is mostly studied by means of optical microscopy [8,9], but the method only reports on the crack closure at the surface. To study the degree of filling within the depth of the crack, X-ray tomography is used [10,11,12]. However, the crack closure does not necessarily indicate that sealing or healing has occurred. A recovery of the water tightness, or self-sealing, is often assessed by water permeability tests [13,14]. Still, to evaluate the regained mechanical performance, mechanical tests are necessary [4,15]. As these testing methods are destructive, the monitoring of the self-healing effectiveness over time is not possible. For this reason, the establishment of a non-destructive testing protocol was initiated, which enables the evaluation of the self-healing properties of cementitious materials.

Thanks to their sensitivity to the elastic properties of a material under study, ultrasonic waves allow to characterize the inner microstructure in a non-destructive manner. The use of ultrasound within cementitious materials ranges from the determination of the setting time [16,17], over the estimation of the mechanical properties [18], to the identification of damage [19,20,21,22]. Linked to the latter topic, recent studies comprised the application of ultrasound to evaluate the repair effectiveness within cementitious mixtures [23,24,25,26,27,28,29]. In these researches, mostly surface wave measurements were described, where emitter and receiver(s) are placed on a single side of the specimen, having the crack in between them. Whereas ultrasound showed to be able to discriminate between the uncracked, cracked and healed stages by means of an analysis of the wave parameters, the information obtained from these measurements concerns a specific zone between the sensors with shallow depth. The characterization capacity is thus limited and the healing effectiveness along the depth as well as within the entire crack volume are not investigated. Nonetheless, variations in the extent of healing are expected, due to the difference in availability of water and CO_2. To eliminate this drawback, in this study ultrasonic mapping by through transmission measurements is applied for the healing evaluation of the entire cross-section. Through transmission has already shown its potential for the characterization of porosity and damage within cementitious materials [30,31,32]. The method consists in measuring characteristics of wave velocity and amplitude at several points along the cross-section, thereby effectively "scanning" the crack volume before and after potential repair action.

In the present study way, the healing effectiveness and the uniformity of the self-healing mechanism along the depth was targeted. Ultrasonic transmission measurements were conducted on cementitious mixtures with and without superabsorbent polymers. Two types of SAP were investigated next to a reference material, in order to evaluate the effect of the SAPs on the self-healing process. The effectiveness not only depends on the overall promotion of autogenous healing, but also concerns the uniformity of healing within the cracked cross-section. Apart from ultrasound experiments, microscopic analysis was performed to assess the visual crack closure and compare with the outcome of the ultrasonic measurements.

2. Materials and methods

2.1. Materials

To investigate the influence of SAPs on the autogenous repair ability and conclude on the ideal type of SAP to be used for self-healing purposes, three mortar mixtures were designed. One of these is a reference material without additives, while the two others contain a different type of superabsorbent polymer. The main constituents comprised a high-strength Portland cement, namely CEM I 52.5 N Strong from Holcim, and river sand 0/2. Sand was added in an amount of 2 to 1 with respect to the weight of the cement. The water-to-cement ratio was equal to 0.35 and a superplasticizer (MasterGlenium 51, BASF) was added in an amount of 0.4 % by weight of cement to increase the workability.

Concerning the mortars with SAPs, an amount of SAPs of 1 % with respect to the weight of cement was introduced. The first type of superabsorbent polymer used was Floset27 CC, obtained from SNF. This SAP is a cross-linked copolymer of acrylamide and acrylic acid with particle sizes between 0 μm and 600 μm. The d_{25}, d_{50} and d_{75} are equal to approximately 180 μm, 250 μm and 320 μm, respectively, while the particle size distribution can be found in [33]. The specific SAP was already investigated in literature and showed an immediate sealing of cracks, as well as an improved healing ability [34,35]. The second SAP is a copolymer of acrylamide and sodium acrylate, called VP 400. This SAP is produced by gel polymerization and was provided by BASF. Whereas the chemical composition is similar compared to Floset27 CC, the particle size is significantly smaller, i.e. d_{50} equal to 70 μm. Its relatively small particle size makes this SAP more ideal for internal curing purposes [36,37,38]. However, previous research demonstrated the beneficial effect of such small SAPs for the improvement of the self-healing capacity of cementitious mixtures [3,5]. To account for the water uptake of the SAPs, additional water was added to the mortar mixtures with SAPs, whilst guaranteeing the same effective water-to-cement ratio as the reference material without SAPs. The exact water quantity to be included was determined by means of a flow table test, following NBN EN 1015–3 [39], so that an identical workability of all fresh mortars was obtained. In case of Floset27 CC, an amount of 20 g additional mixing water per gram of SAP was additionally included, while for VP 400 this was 30 g additional mixing water per gram of SAP. The additional water was added together with the mixing water and dissolved superplasticizer and the SAPs were added to the cement in the dry state.

2.2. Sample preparation

For each mortar composition, one beam measuring 100 mm × 100 mm × 400 mm was cast and cured in plastic foil at 20 ± 2 °C for 28 days. After curing, three slices with a thickness of 50 mm were cut from the middle part of these beams, so to include as little cast surfaces as possible (Fig. 1 (a)). Cracking of the specimens was performed by means of a Brazilian splitting test, shown in Fig. 1 (b), using an Instron 5885H test bench. The splitting test was executed displacement-controlled at a rate of 2 mm/min, leading after cracking to two mortar halves with a thickness of about 25 mm. Subsequently, these parts were reconnected by means of 4 metal tabs (one on each surface), while maintaining an average crack width between 150 μm and 250 μm (see Fig. 2 (a)), as suggested in literature [40].

To promote the healing mechanism, the specimens were placed in wet-dry curing cycles, which consisted of 1 h submersion in water at 20 ± 2 °C and 23 h in dry conditions at 20 ± 2 °C and 60 ± 5 % RH. The specimens were turned over every week, to alternate the position of the microscopic measurement surfaces (facing upward/downward).

2.3. Ultrasonic transmission measurements

The self-healing effectiveness was monitored by ultrasonic transmission measurements, using two piezoelectric sensors of type R15α with a resonance frequency of 150 kHz. The emitter was connected to a waveform generator, which triggered an electric signal of one cycle of 5 V and frequency of 150 kHz. This voltage signal was then transformed by the emitter to a pressure wave that propagated through the mortar specimen. The receiver was placed at the opposite side of the sample, ensuring a travel path between both sensors that was perpendicular to the crack (see Fig. 2). To investigate variations in the healing effectiveness along the cracked cross-section, a grid was drawn on the side surfaces that comprised 25 measuring locations, as shown in Fig. 2 (b). During the ultrasonic assessment, the sensors were moved along this grid, conducting one measurement per position. Vacuum grease was

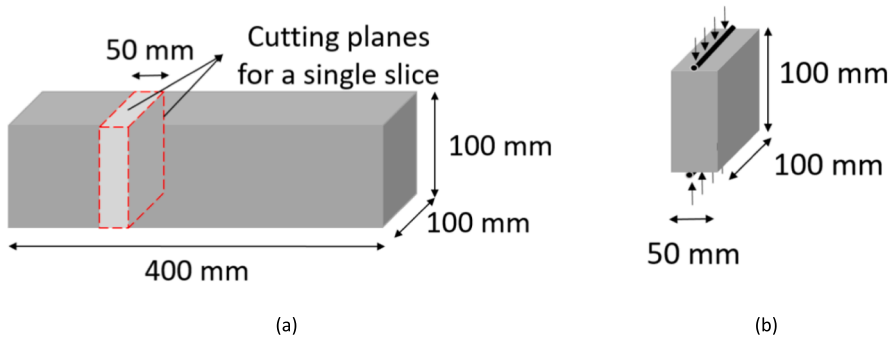

Fig. 1. Schematical representation of (a) sample cutting scheme and (b) Brazilian splitting test.

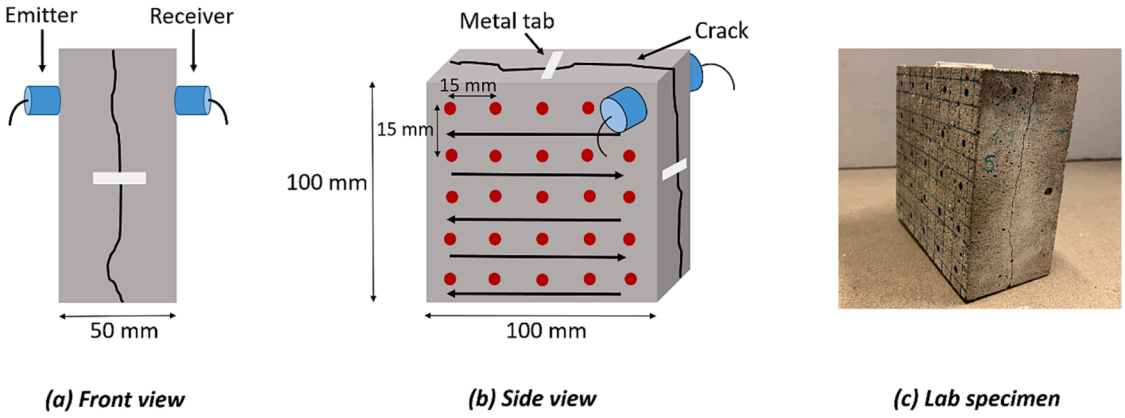

Fig. 2. (a), (b) Schematical representation of the set-up for ultrasonic transmission measurements, revealing the placement of the sensors and the measuring grid and (c) example of a tested specimen.

used to improve the acoustic coupling between the specimen and the sensors. A first set of measurements was performed in the uncracked state and repetitions were executed after cracking (0 days of healing) and after 3, 7, 14 and 28 days of wet-dry curing. As the specimen's degree of saturation might affect the results, the experiments were carried out at the same moment within the wet-dry cycles, i.e. after 16 h of drying.

2.4. Microscopic analysis

The visual crack closure was evaluated by monitoring the crack width openings using an optical microscope. A Leica S8 APO microscope, mounted with a DFC 295 camera was used. Pictures were taken in five locations of the front surface (front view of Fig. 2) and in five locations of the back side. The heights of these locations were aligned with the five lines of the ultrasonic measuring grid. Per picture, five

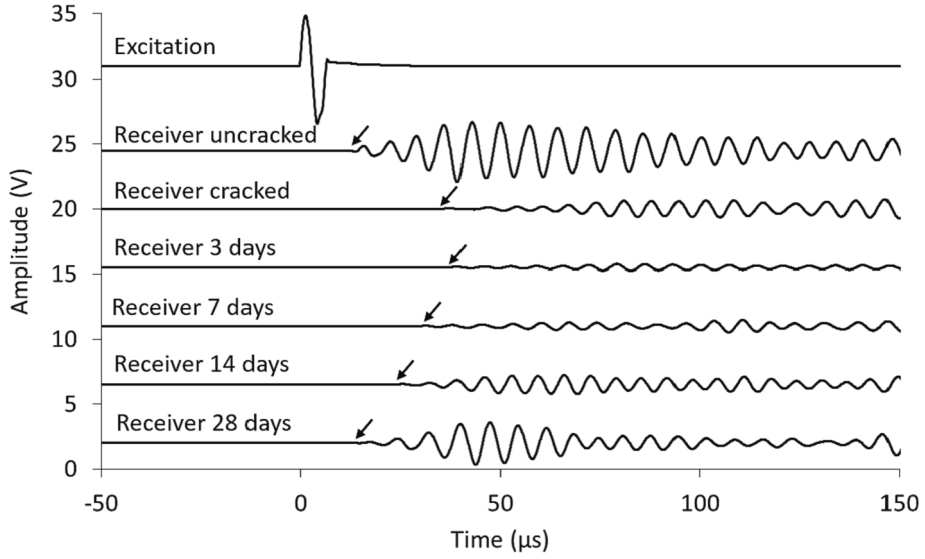

Fig. 3. Evolution of waveforms received over time for a reference specimen. The amplitudes are shifted with respect to their original value, while maintaining their actual shape. The arrows indicate the onset of the waveforms.

measurements of the crack width were carried out, leading to a total of 50 values per specimen. A first analysis was performed immediately after cracking, while repetitions were made after 3, 7, 14 and 28 days of wet-dry curing.

3. Results and discussion

3.1. Raw data

The self-healing capacity was evaluated by analyzing the evolution

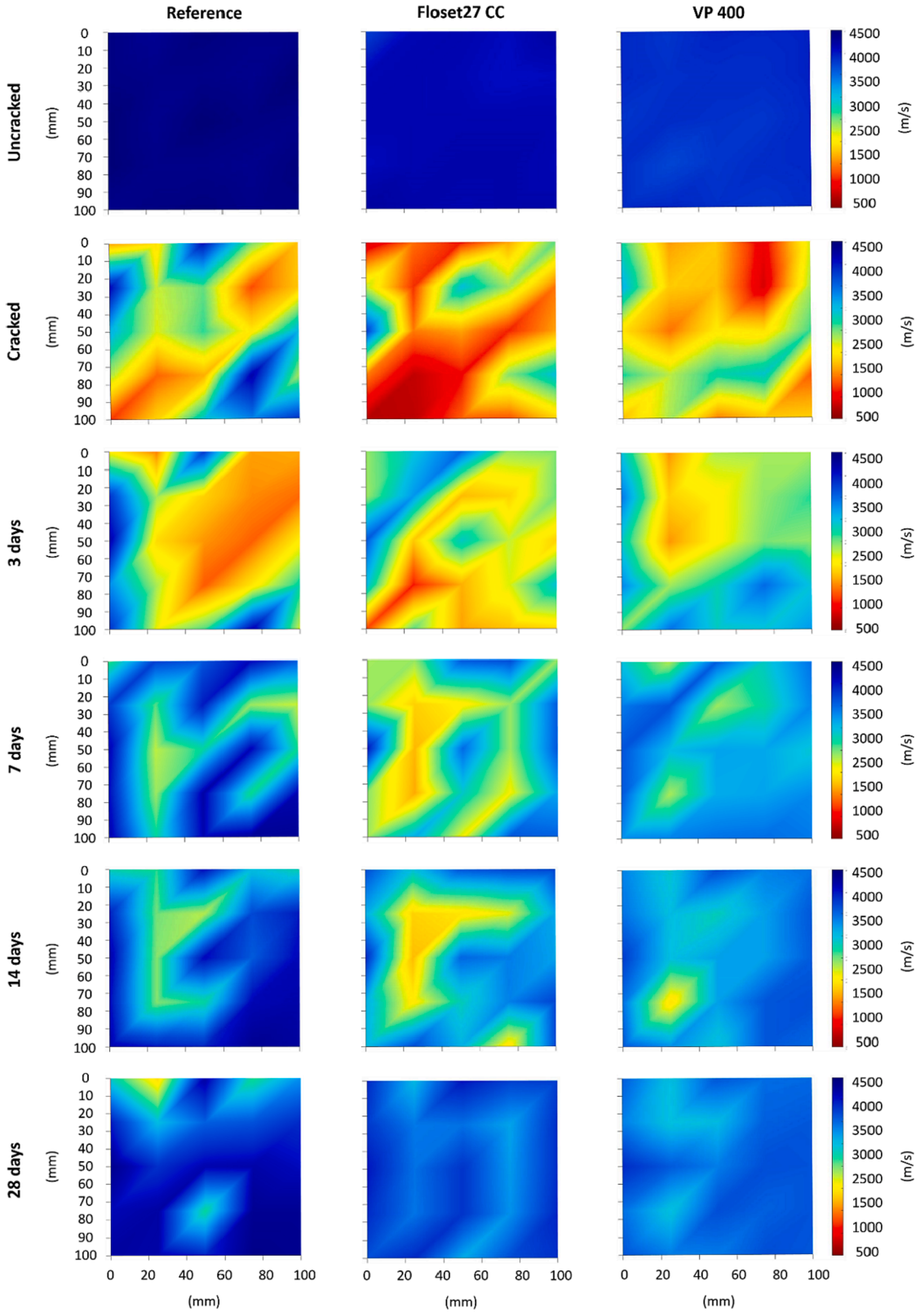

Fig. 4. Evolution of the wave velocity for a representative reference (left), Floset27 CC (middle) and VP 400 (right) specimen over time.

of two wave parameters, namely the wave velocity and the attenuation. To better understand how these parameters enable the self-healing assessment and how they were determined, typical waveforms that were received from a reference specimens are shown in Fig. 3. The excitation signal, sent from the waveform generator, presents a single cycle with onset time at 0 μs. After travelling through the specimen's thickness of 50 mm in the uncracked state, a waveform with reduced amplitude of about 2 V was captured by the receiver. Also, the arrival of the signal, indicated by the first threshold crossing that is defined as the maximum noise level of the received waveform during the "pre-trigger" stage, was delayed compared to the excitation signal, due to the propagation through the specimen thickness. The threshold was stable for all measurements since these were taken with the same acquisition system and it was equal to 5 mV. From these distinct points, different wave parameters were determined. The propagation velocity was calculated by dividing the distance between the sensors (±50 mm) by the time difference between the arrival of the signal at the receiver and the onset time from the excitation signal, after excluding sensor delay effects. For example, a travel time of 12 μs was observed in Fig. 3, which corresponds to a velocity close to 4200 m/s. From the amplitude values, the attenuation of the signal was also calculated. Various factors affect the attenuation, such as the presents of voids, damage, aggregates and the damping of the material itself [41,42]. With x the distance between the sensors and A signifying the amplitude value, the attenuation was calculated using Equation (1):

$$Attenuation\left[\frac{dB}{mm}\right] = -\frac{1}{x}*20*log\left(\frac{A_{receiver}}{A_{emitter}}\right) \quad (1)$$

For comparison purposes, the amplitude of the emitter was taken as the voltage of the electric signal that was fed to the emitter and was constant in all measurements, allowing comparisons between specimens. After cracking, the received waveform showed a significant delay in the onset time, as the crack practically prohibits the wave to travel to the receiving sensor. The arrival of the wave was noticed at approximately 32 μs, leading to a reduced velocity of 1560 m/s. Additionally, the amplitude was also reduced compared to the received signal from the uncracked situation, showing a value of about 0.7 V only. To promote the occurrence of the autogenous healing mechanism, the specimen was placed in wet-dry curing cycles. It can be seen from Fig. 3 that the onset time was advanced over time, in comparison to the cracked state. Also, the amplitude was partially restored, which was clearly visible after 14 and 28 days of healing. The partial recovery of both the wave velocity and the amplitude suggested that partial crack closure had occurred.

3.2. Ultrasonic mapping

In order to investigate the extent of healing within the entire cracked cross-section, a calculation of the wave velocity and attenuation in each of the 25 measuring points was conducted. For reasons of simplicity, only the velocity is detailed within this section, while the attenuation will be shown upon the comparison of the average results in Section 3.3. In Fig. 4, the velocity results are presented by means of color maps. The uncracked situation revealed an approximately uniform velocity distribution for all three specimens. Within the reference specimen, velocities between 4000 and 4500 m/s were reached, which indicate a good quality of the material according to literature [43]. The two samples with SAPs display a slightly lower velocity, i.e. between 3500 and 4000 m/s. This reduction in velocity was caused by the increased macroporosity upon SAP addition. As the SAPs swell during mixing and release the absorbed water after hardening, voids are left behind upon shrinkage of the SAPs [44,17]. Upon crack creation, the velocity lowered significantly within all specimens tested due to the introduced discontinuity. Velocities down to about 500 m/s were calculated in certain areas. Comparing the color maps in the cracked state to the uncracked situation, it can be noticed that the variation in velocity values has strongly increased, leading to a more non-uniform distribution throughout the entire cross-section. This result suggests a variation of the crack width in the cross section of the specimen. Within the cross-section, the gap between the crack walls could differ from the one measured at the sides (nominally 200 μm in average), while bridging points, formed through crushed debris upon reassembly are also possible. The samples were then placed in wet-dry curing cycles for 28 days and repetitions of the ultrasonic measurements were conducted after 3, 7, 14 and 28 days. Regarding the reference specimen, an improvement in velocity within specific zones was noticed, while other locations showed a further degradation after 3 days of healing (Fig. 4 – Reference, 3 days, left). The latter could be caused by the movement of water during wet-dry curing, transporting debris that was previously present within the crack volume. Nonetheless, later assessments demonstrated an increase of the wave velocity over time, meaning that products were deposited inside the crack. Finally, after 28 days of healing, an almost complete recovery of the initial velocity value was obtained in various locations, while other zones still displayed a relatively low velocity between 2500 m/s and 3500 m/s. Similar to the cracking process, the self-healing progress was thus also non-uniform, demonstrating the high characterization potential of ultrasonic mapping to expose variations in the extent of healing.

The evolution of wave velocity within the SAP specimens was comparable to the reference sample. The overall trend, shown in Fig. 4, discloses an improvement of the velocity from 3 to 28 days of wet-dry curing. Again, the healing process occurred in a non-uniform manner, which could in this case also be attributed to the random distribution of SAP particles within the cracked section. After 28 days of healing, a discrepancy between the three mixtures can be distinguished in terms of uniformity. For the reference specimen, the majority of the cross-section exhibited high velocities around 4000 m/s, while there were areas with a lower extent of healing displayed by lower velocity values. While the variation of the measurements is separately treated in a next section (Section 3.3), it is noted that the discrepancy between maximum and minimum was approximately 2500 m/s (from 1890 m/s to 4390 m/s). Regarding Floset27 CC (2nd column of Fig. 4), the distribution of velocities became closer to uniform (max–min discrepancy 1000 m/s) after four weeks of wet-dry curing, meaning that the induced healing process covered the entire cross-section, which would be advantageous in terms of mechanical regain. The sample with SAP VP 400 (3rd column of Fig. 4) showed a behavior amidst the previously described mixtures, but closer to the Floset27 CC case (range 1100 m/s). These results demonstrate the valuable information received from ultrasonic mapping, showing the extent of healing along the interior of a crack through non-destructive testing for the first time in literature. Additionally, the comparison between the different mixtures gives a first indication on the possibility of assessing the uniformity of the healing process within cracked cross-sections.

3.3. Global ultrasonic assessment of the self-healing ability

To allow for a quantitative comparison between the different mixtures, the average wave velocity and average attenuation were calculated from the 25 locations of every specimen for each measuring stage. The coefficients of variation will be detailed later. The evolution of the average wave velocity, presented in Fig. 5 (a), confirms the trends observed from the ultrasonic mapping. In the uncracked situation, represented by the higher values at day 0, a velocity of about 4400 m/s was obtained for the reference specimens. The addition of SAPs to the mortar blends caused an increased macroscopic porosity, leading to a reduction of the wave velocity in both mixtures. After cracking, the wave velocity was considerably lowered on average, due to the introduced discontinuity in the sample. Upon healing, the reference specimens showed a noticeable increase of the wave velocity during the first week. Afterwards, the healing effect slowed down, due to the consumption of

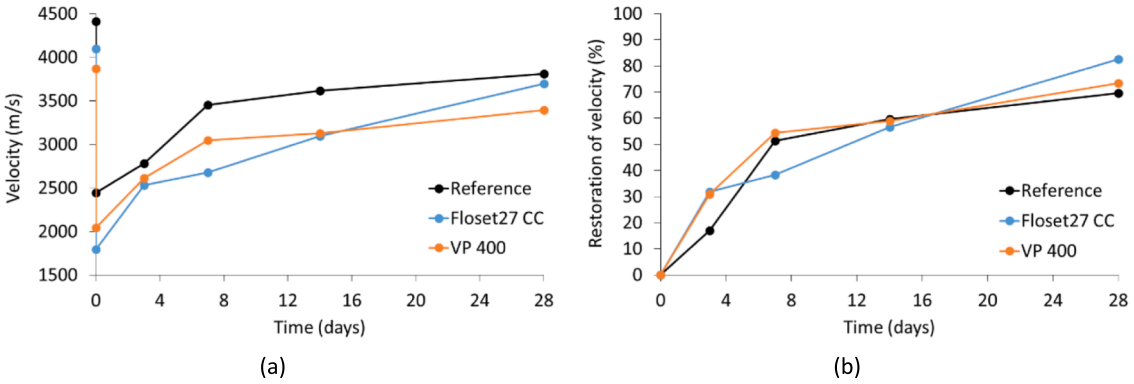

Fig. 5. Evolution of (a) wave velocity and (b) restoration of the wave velocity vs time. The mean evolution between the measuring points is shown as a trend.

unhydrated cement within the cracked cross-section. Similar to the reference, the mixture with VP 400 displayed the largest increase in velocity during the first seven days of wet-dry curing, whereafter only marginal improvements were noticed. Slightly different to these previously discussed mortars, the evolution of the wave velocity was more continuous in case of Floset27 CC addition, suggesting an improvement of the overall healing ability upon inclusion of this particular SAP.

As observed from Fig. 5 (a), the wave velocity partially restored towards the initial value before cracking for all mixtures tested. The restoration of the velocity was calculated in every point and averaged afterwards. Restoration was defined as the parameter's gain between the cracked and the healed stages divided by the reduction of this parameter due to cracking, and was calculated by means of Equation (2):

$$Restoration[\%] = \frac{Q_{healed} - Q_{cracked}}{Q_{uncracked} - Q_{cracked}} * 100 \quad (2)$$

where Q_X signifies the value of the parameter under study, namely the velocity or the attenuation, at stage X (uncracked, cracked or healed). The average parameter values, e.g. as depicted in Fig. 5 (a) for the velocity, were used for this calculation. Fig. 5 (b) depicts the average restoration of the velocity for all three mixtures over time. Regarding the reference, a restoration of 17 % was obtained after three days of wet-dry curing, which was considerably smaller than the recovery for the SAP blends. Afterwards, the restoration percentage increased and a final value of 70 % was reached at 28 days of healing. Upon the inclusion of VP 400 a recovery of 31 % was found within the first three days, demonstrating the improved water storage through SAPs. Between three and seven days, the restoration started to slow down and eventually, during the last three weeks, a similar evolution compared to the reference was seen. The final restoration value of VP 400 mortar was equal to 73 %, revealing once again the promoted healing ability. Lastly, the mixtures with Floset27 CC showed a similar recovery from the start compared to VP 400, whereas the restoration clearly slowed down between three and seven days of healing. However, the recovery developed more continuously at later healing ages, which led to the highest restoration value (i.e. 83 %) of all three mixtures. This outcome confirms the trends observed in literature, where larger sizes of SAPs proved to be more efficient for self-healing purpose [45,46]. However, it should be mentioned that many more SAP characteristics, like the chemistry and water kinetics, affect the healing capacity.

In Fig. 6 (a) the average attenuation is plotted with respect to the time. When comparing the attenuation between the various mixtures, it was noticed that the values for reference and VP 400 specimens were closely related in the uncracked state, while the attenuation was much higher for Floset27 CC addition. Similar to the reduced wave velocity, this was attributed to the presence of macropores, increasing the scattering attenuation of the wave. Afterwards, the introduction of the crack posed a discontinuity within the matrix, which strongly increased the attenuation of all mortars. The effect of the crack was more pronounced within the mixtures with SAPs, compared to the reference, suggesting larger average crack widths within these specimens. From the onset of the wet-dry curing cycles onwards, a partial restoration of the average attenuation was noticed for all mixtures under study. A noticeable decrease in attenuation of the reference blends was only observed between three and seven days of healing. The mortars with SAPs showed a strong recovery in attenuation from the start of healing, which slowed down after seven days in case of VP 400, while for Floset27 CC a more continuous decreasing trend was maintained until the end of wet-dry curing.

The restoration percentages in terms of attenuation are shown in Fig. 6 (b). The evolution of the attenuation's restoration was practically identical for the SAP mortars during the first two weeks of healing. Afterwards, the Floset27 CC specimens demonstrated a continued recovery like in the case of wave velocity, giving rise to a final average recovery of

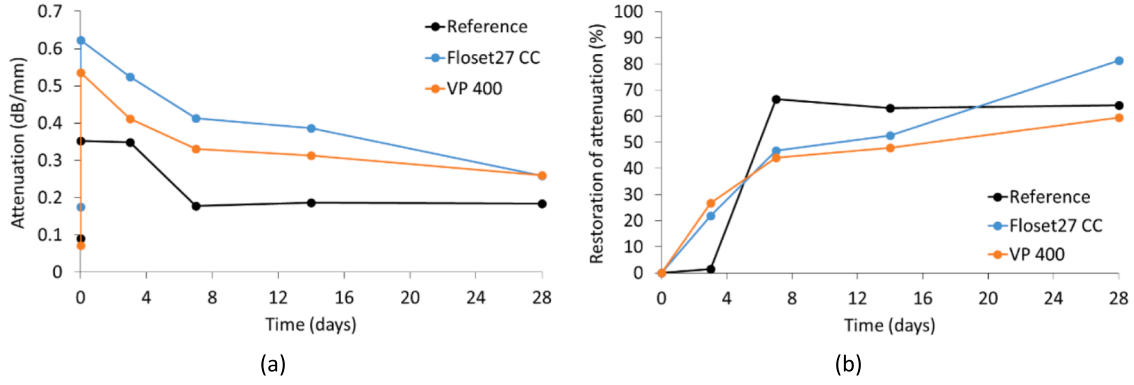

Fig. 6. Evolution of (a) attenuation and (b) restoration of attenuation vs time. The mean evolution between the measuring points is shown as a trend.

81 %. For the reference mixture, the healing mechanism was mostly evident between three and seven days, while afterwards no further improvement could be distinguished. After 28 days of wet-dry curing, similar restorations of 64 % and 59 % were obtained for reference and VP 400, respectively. Hence, it was seen that the use of non-destructive ultrasonic measurements enabled an assessment of the overall self-healing capacity of cementitious mixtures and allowed to distinguish between various mix designs.

As explained in Section 3.2, the use of ultrasonic mapping allowed to evaluate the extent of healing along the entire cross-section and thus to assess the uniformity of the healing mechanism. For this reason, the coefficients of variation (COV), being the standard deviations on the average results divided by the average values, were calculated for the wave velocity at all measurement stages. In Fig. 7, negligibly small values around 1 % were received in the uncracked state for all mixtures, which confirms the uniform distribution of the velocity values as depicted in Fig. 4. The cracking process largely increased the variation on the results, as the crack widths vary between different locations, while random bridging points are also possible. In all cases, the COV increased to more than 30 %. The application of wet-dry curing cycles, promoting the autogenous healing process, also showed to reduce the COV on the wave velocity over time, apart from increasing the velocity as discussed above. A comparison between the different mixtures revealed a discrepancy between the reference and SAP mixes, namely the higher decrease in COV upon SAP addition. While a value of 21 % was obtained after 28 days for the reference material, the SAP blends reached a value of 7 to 8 %, suggesting a promotion of the uniformity of healing on top of the overall improved healing ability.

It is mentioned that, while possible coupling variations may influence the measurement of amplitude by 20 % (and according to Eq. (1), the attenuation by approximately 0.03 dB/mm), the influence on transit time is much smaller (less than 0.2 μs or approximately 1 % of the absolute value), provided that the signal is strong enough to identify the onset of the first cycle above the noise level. This possible attenuation variation of 0.03 dB/mm is much smaller than the change due to material condition. Indeed, cracking increases the attenuation in average from 0.1 to 0.5 dB/mm, while healing decreases attenuation back to about 0.25 dB/mm. Therefore, while attenuation is still a sufficiently sensitive measure to indicate the large changes due to material condition (cracking/healing), concerning the point to point uniformity within each healing stage, it was chosen to focus on the aforementioned velocity variation, since possible coupling influence is an order of magnitude smaller.

3.4. Microscopic analysis

The visual crack closure was assessed by means of microscopic analysis. Per specimen, 50 crack width measurements were conducted in the cracked and healed stages. To get an idea of the information obtained from microscopic analysis, Fig. 8 shows the evolution of one random crack location per mortar mixture from immediately after cracking to 14 and 28 days of wet-dry curing. For each mixture tested, a whitish product is deposited inside the crack, which leads to a reduction of the average crack width over time.

In Fig. 9, the average of all measurements of a mixture series is plotted with respect to the time. The standard deviations on these values can be found in Table 1 in Appendix. Immediately after cracking, the two parts of one specimen were reassembled by pushing the halves together and measuring the crack width in few locations to obtain a size between 150 μm and 250 μm. Whereas for all samples the target crack width was approximately achieved, differences in crack size between various locations and specimens were inevitably present (see Appendix Table 1). The average crack width of reference specimens was equal to 171 μm, while for the SAP mortars a relatively larger crack width around the upper limit of 250 μm was resulted. Whereas the microscopic pictures only provided information on the crack width openings at the surface, these higher average values also suggest a general increase of the distance between the crack walls. This noticeable difference between reference and SAP specimens explains the variations encountered during the analysis of the wave velocity and attenuation, namely a reduction in wave velocity and an increase in attenuation for the mortars with superabsorbent polymers after cracking. Afterwards, the specimens were placed in wet-dry curing cycles and the average crack width decreased over time for all mixtures tested. After 28 days of healing, the reference and VP 400 samples demonstrated an almost identical average crack size just below 60 μm. For Floset27 CC, a higher value of 93 μm was found.

As the initial crack widths differed between the various mixtures, a relative measurement of the visual healing ability with respect to the initial crack width is relevant. For this reason, the healing ratio at the distinct stages was calculated using Eq. (3), where CW signifies the crack width at stage X (cracked or healed).

$$Healingratio[\%] = \frac{CW_{cracked} - CW_{healed}}{CW_{cracked}} * 100 \quad (3)$$

From Fig. 9 (b), it can be seen that the reference and VP 400 mortars showed a similar visual healing ratio after three days of wet-dry curing,

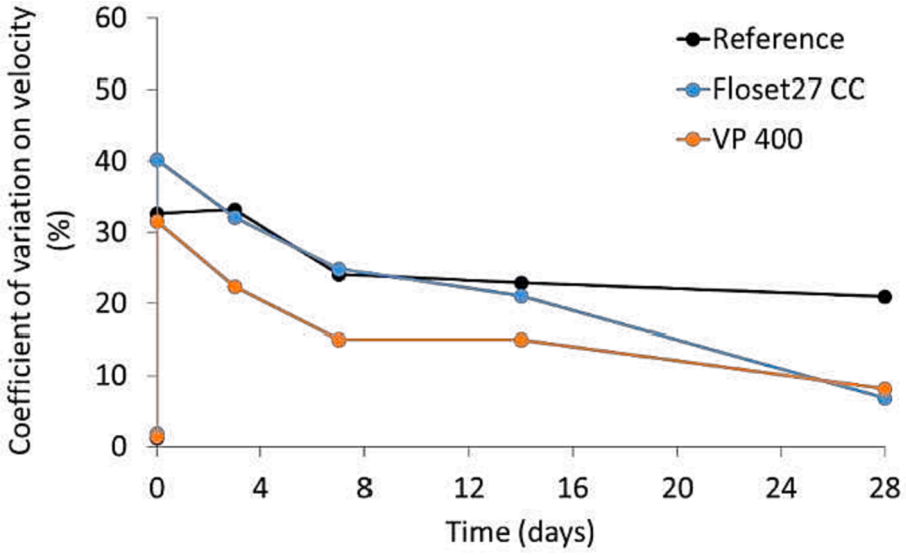

Fig. 7. Coefficient of variation on the average wave velocity vs time.

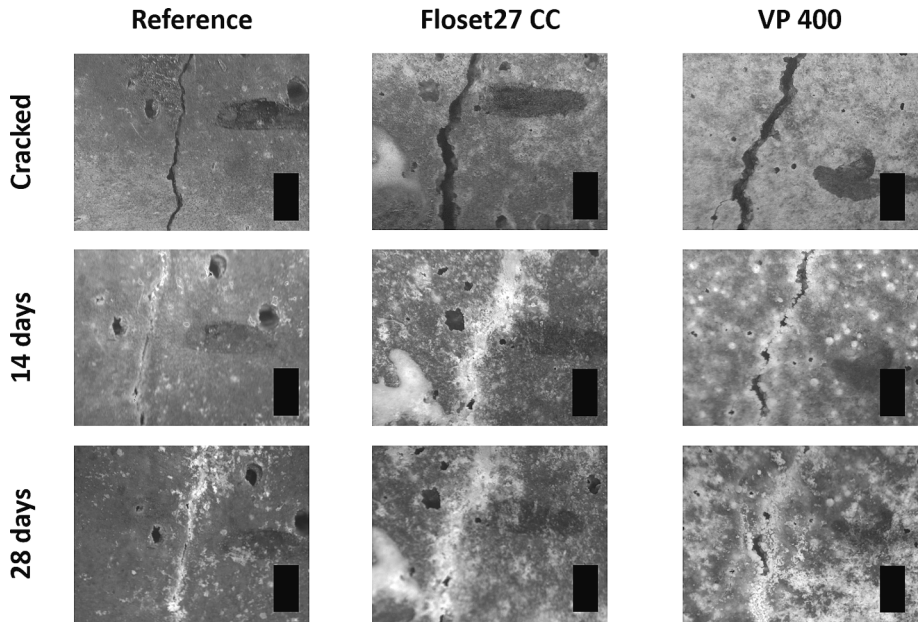

Fig. 8. Representative examples of microscopic crack width pictures after cracking and after 14 and 28 days in wet-dry curing cycles. The black rectangles have a height of 1000 μm.

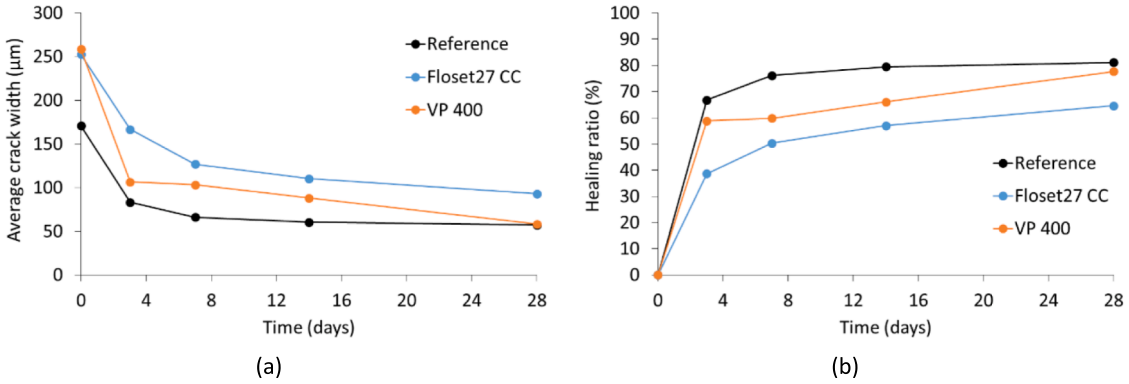

Fig. 9. Evolution of (a) average crack width and (b) healing ratio vs time after microscopic analysis. The mean evolution between the measuring points is shown as a trend.

which was significantly higher compared to the Floset27 CC mixture. Afterwards, the increasing trend slowed down for all mortars. At the end of the healing period, Floset27 CC demonstrated the lowest healing visual ratio, equal to 65 %, whereas this material displayed the best results in terms of global restoration of the ultrasonic parameters. These results thus indicate the possible difference between the crack closure at the surface and the crack filling within deeper layers and confirm the necessity of a measuring technique that evaluates the entire cracked cross-section. Additionally, it should be noted that, as the average initial crack widths were not identical between the mixtures (range from 150 μm to 250 μm), this could affect the healing progress as well. For this reason, the evolution of the average crack width of three separate specimens, i.e. one of each mixture, with similar initial crack width are plotted in Fig. 10 (a). The specific specimens, as referred to in Appendix Table 1, are Reference 3, Floset27 CC 3 and VP 400 1. Starting from similar crack sizes, the reference and Floset27 CC samples followed an identical trend during the first three days, while an evident improvement of the crack closure was seen for VP 400. Eventually, the largest average crack width at 28 days of healing was measured for the reference, equal to 135 μm. The inclusion of SAPs led to a reduced average crack width, being 75 μm and 42 μm for Floset27 CC and VP 400 respectively, confirming the promoted healing ability.

As a means of comparison, the evolution of the wave velocity of these specific specimens is presented in Fig. 10 (b). While similar initial crack widths were measured, a clear discrepancy in wave velocity values was seen after cracking, which indicated the shortcoming of the microscopic analysis that only provides information on the crack filling at the surface. During healing, the velocity developments were closely related between the three specimens. Finally, after 28 days, the lowest velocity was obtained for the reference blend, while the SAP mortars revealed an improvement of the healing ability.

It is characteristic that based on surface applied microscopy inspection of the crack width, the VP 400 SAPs series indicated the highest restoration when similar initial crack widths were compared between mixture series, but when the internal part of the crack was assessed through ultrasound the results consistently show higher restoration with the Floset27 CC. The latter outcome demonstrates the difference between healing along the crack depth and healing at the surface. The self-healing capacity of the reference material was lower compared to the SAP blends.

Lastly, a correlation between the visual crack closure and the ultrasonic measurements was examined. Whereas the microscopic analysis

Table 1
Average crack width [μm] and standard deviation [μm] per specimen and per mixture design.

		Cracked	3 days	7 days	14 days	28 days
Reference	Specimen 1	169 ± 59	73 ± 94	49 ± 96	49 ± 100	39 ± 82
	Specimen 2	102 ± 36	11 ± 26	9 ± 26	0 ± 0	0 ± 0
	Specimen 3	241 ± 109	169 ± 135	148 ± 142	136 ± 142	135 ± 137
	Total average	171 ± 92	83 ± 114	66 ± 113	61 ± 114	57 ± 107
Floset27 CC	Specimen 1	251 ± 37	145 ± 105	126 ± 100	104 ± 92	93 ± 89
	Specimen 2	268 ± 37	180 ± 100	133 ± 106	132 ± 112	111 ± 116
	Specimen 3	236 ± 64	170 ± 87	121 ± 93	92 ± 98	75 ± 94
	Total average	253 ± 49	167 ± 98	127 ± 99	110 ± 102	93 ± 102
VP 400	Specimen 1	236 ± 57	92 ± 78	91 ± 79	72 ± 72	42 ± 71
	Specimen 2	290 ± 49	140 ± 119	134 ± 115	116 ± 108	93 ± 107
	Specimen 3	257 ± 43	93 ± 102	92 ± 92	80 ± 91	44 ± 75
	Total average	259 ± 54	106 ± 101	103 ± 96	88 ± 92	58 ± 87

revealed the filling of the cracks at the outer surfaces, ultrasonic experiments were conducted throughout the whole cross-section. As the latter measurements were not performed in exactly the same locations as used during microscopy, a direct link between the crack widths and the velocity or attenuation values at a specific location would not be valid. Therefore, it was chosen to compare the average crack width per mixture series, as measured by microscopy in all 10 locations on the front and back surfaces of the three specimens, to the average velocity and attenuation per mixture series. In Fig. 11 (a), the average velocity measured at different healing ages is plotted with respect to the average crack width of all investigated samples. While the average velocity values concern the entire crack volume and the crack widths solely provide information about the crack opening at the surface, a negative correlation between velocity and crack widths was observed. In the uncracked stage (crack width equal to zero), all average velocities showed a value above 3500 m/s, whereas in case of crack sizes above 200 μm, measured immediately after cracking, the velocity decreased to 2500 m/s or less. In between these two extreme cases, an increase of velocity with decreasing crack widths was obtained, which demonstrated the sensitivity of ultrasound to the healing process.

The average attenuation vs crack width is presented in Fig. 11 (b), where an opposite trend compared to the velocity can be noticed. For intact specimens, the attenuation was limited below 0.2 dB/mm, while after cracking, when crack widths of about 200 μm were exhibited, attenuation increased to approximately 0.6 dB/mm. With decreasing crack width during the healing cycles, a decrement of the average attenuation was observed, indicating the sensitivity of wave transmission both to the initial cracking and to the healing process. However, it is reminded that a one-on-one correlation cannot be performed, due to the difference in measuring locations between the two adopted techniques. Additionally, microscopic analysis indicated the closure of cracks, but this does not imply a stiff connection between the crack walls, something that can be confirmed only by ultrasonic measurements.

It should be emphasized that the differences caught by ultrasound are driven by the change in the very thin layer of the crack (of

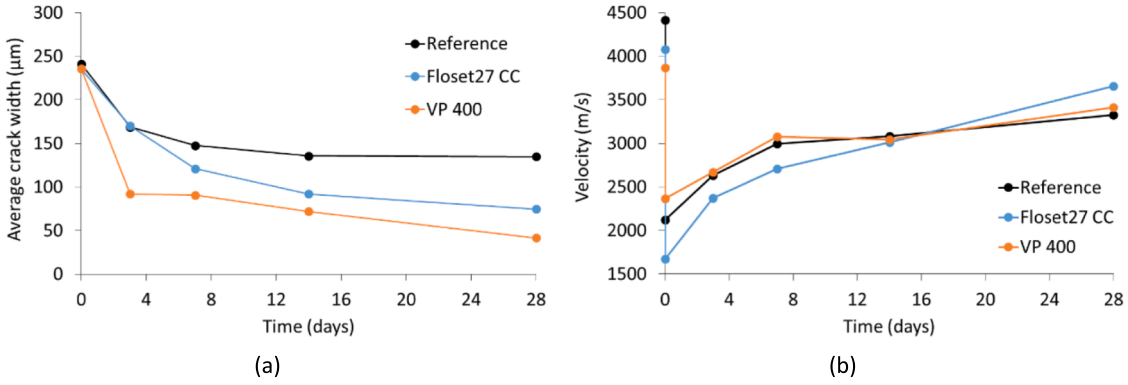

Fig. 10. Evolution of (a) average crack width and (b) wave velocity of three specimens with similar initial crack widths.

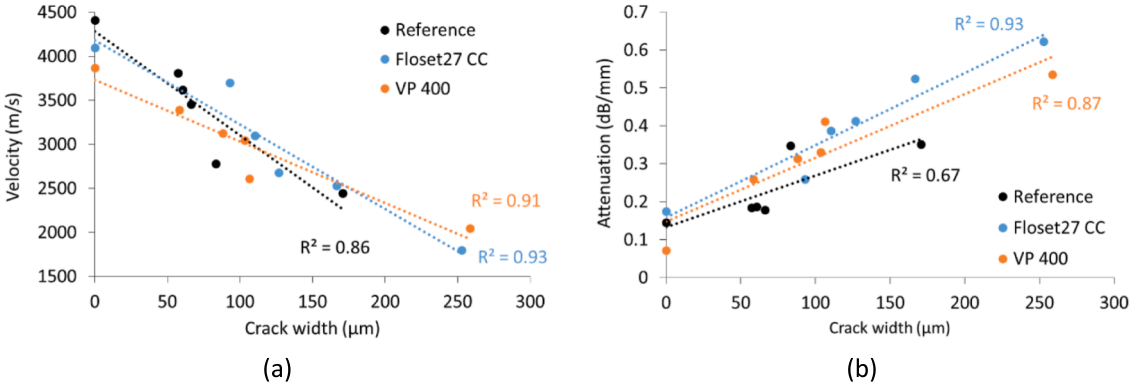

Fig. 11. (a) Average velocity and (b) average attenuation vs average crack width, measured at different healing ages.

approximately 200 μm) as the rest of the path at either sides of the crack is not expected to be much influenced. This shows the sensitivity of elastic waves to changes even on the microscopic level, due to the physical propagation through the material of interest. In addition, it will make the effort for evaluation of the mechanical properties of the healing materials in the crack possible, since the only change is concentrated inside the crack and the properties of the rest of the path are known. The sensitivity of ultrasound enables a global assessment of the self-healing capacity, while for the first time it provides information on the interior of the crack away from the surface. It also allows possible automatic scanning that can offer more resolution in space. This opens the way for a realistic, detailed assessment of the self-healing performance, first in laboratory conditions in order, for example, to select the best SAPs for more effective and more uniform healing inside the whole volume of the crack, and second with possible modifications (e.g. excitation frequency, grid) in real size structural members.

4. Conclusions

The self-healing ability of three cementitious mortars, namely-one reference material and two mixtures with different superabsorbent polymers, was investigated by means of ultrasonic transmission measurements and microscopic analysis. Autogenous healing was promoted by the application of wet-dry curing cycles.

In the uncracked situation, ultrasound revealed the higher porosity of the mortars with SAPs by a lower velocity and higher attenuation. Upon cracking, a significant decrease of the velocity and an increase of the attenuation was evident for all mixtures. The application of wet-dry curing cycles caused a partial restoration of these parameters over time, as healing products were deposited inside the cracks. Through the calculation of the restoration percentage, the beneficial effect of SAP inclusion for self-healing purpose was confirmed. A comparison between the two types of SAP exposed a significantly higher recovery of the velocity for Floset27 CC, having a larger particle size, allowing to compare different SAPs' ability to promote self-healing. Moreover, the adoption of through-transmission ultrasound enabled an assessment of the entire cross-section and displayed variations in the extent of healing along the depth. From these results, the use of SAPs suggested an increase of the uniformity of the healing process by a reduction of the coefficient of variation of velocity at different points of the cross section.

By means of microscopic analysis, the visual crack closure at the surface was evaluated. Consecutive measurements of the crack width indicated the filling of the cracks during wet-dry curing for all materials tested. Through the calculation of the healing ratio, a comparison between the different mixtures was conducted and demonstrated a strong improvement in the visual crack closure for the VP 400 mortar compared to the other blends. Also, a correlation between the average crack width and the average velocity and attenuation was revealed. While the inclusion of Floset27 CC showed the smallest healing ratio from microscopic analysis, ultrasonic measurements exposed the highest recovery in terms of velocity for this mixture as well as an increased uniformity of the healing process through the cross-section. These results therefore validate the importance of assessing the self-healing capacity along the entire cracked cross-section over a superficial microscopic evaluation. The through-the-thickness application of ultrasound provided indicative information on the extent of healing and the uniformity of the process along the depth in a non-destructive manner.

CRediT authorship contribution statement

Gerlinde Lefever: Methodology, Formal analysis, Investigation, Writing – original draft, Visualization. **Danny Van Hemelrijck:** Conceptualization, Methodology, Validation, Writing – review & editing, Supervision. **Dimitrios G. Aggelis:** Conceptualization, Methodology, Validation, Writing – review & editing, Supervision. **Didier Snoeck:** Conceptualization, Methodology, Validation, Writing – review & editing, Supervision.

Declaration of Competing Interest

The authors declare that they have no known competing financial interests or personal relationships that could have appeared to influence the work reported in this paper.

Data availability

Data will be made available on request.

Acknowledgements

This research is funded by the Vrije Universiteit Brussel through an OZR backup mandate (OZR3776). The financial support is therefore gratefully acknowledged by all authors. The authors also wish to express their gratitude to Dr. Alexander Assmann (BASF) and Mr. Guillaume Jeanson (SNF) for providing the SAPs under study.

References

[1] H. Huang, G. Ye, C. Qian, E. Schlangen, Self-healing in cementitious materials: Materials, methods and service conditions, Mater. Des. 92 (2016) 499–511.
[2] N. De Belie, E. Gruyaert, A. Al-Tabbaa, P. Antonaci, C. Baera, D. Bajare, A. Darquennes, R. Davies, L. Ferrara, T. Jefferson, C. Litina, B. Miljevic, A. Otlweska, J. Ranogajec, M. Roig-Flores, K. Paine, P. Lukowski, P. Serna, J.-M. Tulliani, S. Vucetic, J. Wang, H. Jonkers, A review of self-healing concrete for damage management of structures, Adv. Mater. Interfaces 5 (17) (2018) 1800074.
[3] D. Snoeck, N. De Belie, Autogenous healing in strain-hardening cementitious materials with and without superabsorbent polymers: an 8-year study, Front. Mater. 6 (48) (2019) 1–12.
[4] D. Snoeck, N. De Belie, Repeated autogenous healing in strain-hardening cementitious composites by using superabsorbent polymers, J. Mater. Civ. Eng. 28 (1) (2015) 04015086.
[5] G. Lefever, D. Snoeck, D. Aggelis, N. De Belie, S. Van Vlierberghe, D. Van Hemelrijck, Evaluation of the self-healing ability of mortar mixtures containing superabsorbent polymers and nanosilica, Materials 13 (2) (2020) 380.
[6] G. Hong, C. Song, S. Choi, Autogenous healing of early-age cracks in cementitious materials by superabsorbent polymers, Materials 13 (3) (2020) 690.
[7] C. Schröfl, K. Erk, W. Siriwatwechakul, M. Wyrzykowski, D. Snoeck, Recent progress in superabsorbent polymers for concrete, Cem. Concr. Res. 151 (2022), 106648.
[8] L. Ferrara, T. Van Mullem, M. Cruz Alonso, P. Antonaci, R. Borg, E. Cuenca, A. Jefferson, P.-L. Ng, A. Peled, M. Roig-Flores, M. Sanchez, C. Schröfl, P. Serna, D. Snoeck, J. Tulliani, N. De Belie, Experimental characterization of the self-healing capacity of cement based materials and its effects on the material performance: A state of the art report by COST Action SARCOS WG2, Constr. Build. Mater. 167 (2018) 115–142.
[9] A. Suleiman, A. Nelson, M. Nehdi, Visualization and quantification of crack self-healing in cement-based materials incorporating different minerals, Cem. Concr. Compos. 103 (2019) 49–58.
[10] J. Wang, J. Dewanckele, V. Cnudde, S. Van Vlierberghe, W. Verstraete, N. De Belie, X-ray computed tomography proof of baterial-based self-healing in concrete, Cem. Concr. Compos. 53 (2014) 289–304.
[11] D. Snoeck, J. Dewanckele, V. Cnudde, N. De Belie, X-ray computed microtomography to study autogenous healing of cementitious material promoted by superabsorbent polymers, Cem. Concr. Compos. 65 (2016) 83–93.
[12] A. Sidiq, R. Gravina, S. Setunge, F. Giustozzi, High-efficiency techniques and micro-structural parameters to evaluate concrete self-healing using X-ray tomography and Mercury Intrusion Porosimetry: A review, Constr. Build. Mater. 252 (2020), 119030.
[13] J. Wang, H. Soens, W. Verstraete, N. De Belie, Self-healing concrete by use of microencapsulated bacterial spores, Cem. Concr. Res. 56 (2014) 139–152.
[14] T. Van Mullem, E. Gruyaert, B. Debbaut, R. Caspeele, N. De Belie, Novel active crack width control technique to reduce the variation on water permeability results for self-healing concrete, Constr. Build. Mater. 203 (2019) 541–551.
[15] S. Qian, J. Zhou, M. de Rooij, E. Schlangen, G. Ye, K. van Breugel, Self-healing behavior of strain hardening cementitious composites incorporating local waste materials, Cem. Concr. Compos. 31 (9) (2009) 613–621.
[16] N. De Belie, C. Grosse, J. Kurz, H. Reinhardt, Ultrasound monitoring of the influence of different accelerating admixtures and cement types for shotcrete on setting and hardening behaviour, Cem. Concr. Res. 35 (2005) 2087–2094.
[17] G. Lefever, D. Aggelis, N. De Belie, M. Raes, T. Hauffman, D. Van Hemelrijck, D. Snoeck, The influence of superabsorbent polymers and nanosilica on the hydration process and microstructure of cementitious mixtures, Materials 13 (22) (2020) 5194.

[18] F. Silva, J. Delgado, R. Cavalcanti, A. Azevedo, A. Guimaraes, A. Lima, Use of nondestructive testing of ultrasound and artificial neural networks to estimate compressive strength of concrete, Buildings 11 (2) (2021) 44.
[19] J.-F. Chaix, V. Garnier, G. Corneloup, Ultrasonic wave propagation in heterogeneous solid media: Theoretical analysis and experimental validation, Ultrasonics 44 (2) (2006) 200–210.
[20] P. Antonaci, C. Bruno, A. Gliozzi, M. Scalerandi, Monitoring evolution of compressive damage in concrete with linear and nonlinear ultrasonic methods, Cem. Concr. Res. 40 (7) (2010) 1106–1113.
[21] M. Ohtsu, Elastic wave methods for NDE in concrete based on generalized theory of acoustic emission, Constr. Build. Mater. 122 (2016) 845–854.
[22] E. Ahn, M. Shin, J. Popovics, R. Weaver, Effectiveness of diffuse ultrasound for evaluation of micro-cracking damage in concrete, Cem. Concr. Res. 124 (2019), 105862.
[23] D. Aggelis, T. Shiotani, Repair evaluation of concrete cracks using surface and through-transmission wave measurements, Cem. Concr. Compos. 29 (9) (2007) 700–711.
[24] D. Aggelis, T. Shiotani, D. Polyzos, Characterization of surface crack depth and repair evaluation using Rayleigh waves, Cem. Concr. Compos. 31 (1) (2009) 77–83.
[25] R. Alghamri, A. Kanellopoulos, A. Al-Tabbaa, Impregnation and encapsulation of lightweight aggregates for self-healing concrete, Constr. Build. Mater. 124 (2016) 910–921.
[26] E. Ahn, H. Kim, S. Sim, S. Shin, M. Shin, Principles and applications of ultrasonic-based nondestructive methods for self-healing in cementitious materials, Materials 10 (3) (2017) 278.
[27] A. Gliozzi, M. Scalerandi, G. Anglani, P. Antonaci, L. Salini, Correlation of elastic and mechanical properties of consolidated granular media during microstructure evolution induced by damage and repair, Physical review materials 2 (2018), 013601.
[28] E. Tsangouri, J. Lelon, P. Minnebo, H. Asaue, T. Shiotani, K. Van Tittelboom, N. De Belie, D. Aggelis, D. Van Hemelrijck, Feasibility study on real-scale, self-healing concrete slab by developing a smart capsules network and assessed by a plethora of advanced monitoring techniques, Constr. Build. Mater. 228 (2019), 116780.
[29] G. Lefever, D. Snoeck, N. De Belie, S. Van Vlierberghe, D. Van Hemelrijck, D. Aggelis, The contribution of elastic wave NDT to the characterization of modern cementitious media, Sensors 20 (10) (2020) 2959.
[30] V. Haach, F. Ramirez, Qualitative assessment of concrete by ultrasound tomography, Constr. Build. Mater. 119 (2016) 61–70.
[31] M. Zielinska, M. Rucka, Non-destructive assessment of masonry pillars using ultrasonic tomography, Materials 11 (12) (2018) 2543.
[32] T. Shiotani, S. Momoki, H. Chai, D. Aggelis, Elastic wave validation of large concrete structures repaired by means of cement grouting, Constr. Build. Mater. 23 (7) (2009) 2647–2652.
[33] C. Rodriquez, M. Deprez, F. Mendonca Filho, S. Offenwert, V. Cnudde, E. Schlangen, B. Savija, X-ray micro tomography of water absorption by superabsorbent polymers in mortar, vol. Nov. 25, in: International Conference on Application of Superabsorbent Polymers & Other New Admixtures Towards Smart Concrete, 2019, pp. 29–37.
[34] E. Gruyaert, B. Debbaut, D. Snoeck, P. Diaz, A. Arizo, E. Tziviloglou, E. Schlangen, N. De Belie, Self-healing mortar with pH-sensitive superabsorbent polymers: testing of the sealing efficiency by water flow tests, Smart Mater. Struct. 25 (8) (2016), 084007.
[35] J. Pelto, M. Leivo, E. Gruyaert, B. Debbaut, D. Snoeck, N. De Belie, Application of encapsulated superabsorbent polymers in cementitious materials for stimulated autogenous healing, Smart Mater. Struct. 26 (2017), 105043.
[36] D. Snoeck, L. Pel, N. De Belie, The water kinetics of superabsorbent polymers during cement hydration and internal curing visualized and studied by NMR, Sci. Rep. 7 (9514) (2017) 1–14.
[37] D. Snoeck, W. Goethals, J. Hovind, P. Trtik, T. Van Mullem, P. Van den Heede, N. De Belie, Internal curing of cement pastes by means of superabsorbent polymers visualized by neutron tomography, Cem. Concr. Res. 147 (2021), 106528.
[38] G. Lefever, D. Snoeck, N. De Belie, D. Van Hemelrijck, D. Aggelis, Elastic wave monitoring of cementitious mixtures including internal curing mechanisms, Sensors 21 (2021) 2463.
[39] Belgisch instituut voor normalisatie (BIN), *Methods of test for mortar masonry - Part 3: Determination of consistence of fresh mortar (by flow table)*, 1999.
[40] K. Van Tittelboom, N. De Belie, Self-healing in cementitious materials - A review, Materials 6 (2013) 2182–2217.
[41] L. Jacobs, J. Owino, Effect of aggregate size on attenuation of Rayleigh surface waves in cement-based materials, J. Eng. Mech. 126 (11) (2000) 1124–1130.
[42] T.P. Philippidis, D.G. Aggelis, Experimental study of wave dispersion and attenuation in concrete, Ultrasonics 43 (7) (2005) 584–595.
[43] T. Naik, V. Malhotra, J. Popovics, The ultrasonic pulse velocity method, in: V. Malhotra, N. Carino (Eds.), Handbook on Nondestructive Testing of Concrete, second ed., CRC Press, 2003, pp. 8-1–8-19.
[44] B. Olawuyi, W. Boshoff, Influence of SAP content and curing age on air void distribution of high performance concrete using 3D volume analysis, Constr. Build. Mater. 135 (2017) 580–589.
[45] D. Snoeck, S. Steuperaert, K. Van Tittelboom, P. Dubruel, N. De Belie, Visualization of water penetration in cementitious materials with superabsorbent polymers by means of neutron radiography, Cem. Concr. Res. 42 (8) (2012) 1113–1121.
[46] D. Snoeck, K. Van Tittelboom, S. Steuperaert, P. Dubruel, N. De Belie, Self-healing cementitious materials by the combination of microfibres and superabsorbent polymers, J. Intell. Mater. Syst. Struct. 25 (1) (2014) 13–24.